Zinc Finger Protein5 Is Required for the Control of Trichome Initiation by Acting Upstream of *Zinc Finger Protein8* in Arabidopsis[1[C][W][OA]]

Zhongjing Zhou[2], Lijun An[2], Lili Sun, Shuijin Zhu, Wanyan Xi, Pierre Broun, Hao Yu, and Yinbo Gan*

Department of Agronomy, College of Agriculture and Biotechnology, Zhejiang University, Hangzhou 310058, China (Z.Z., L.A., L.S., S.Z., Y.G.); Nestlé R&D Center Tours, Plant Science and Technology, 37390 Notre Dame d'Oé, France (P.B.); and Department of Biological Sciences and Temasek Life Sciences Laboratory, National University of Singapore, 117543 Singapore (W.X., H.Y.)

Arabidopsis (*Arabidopsis thaliana*) trichome development is a model system for studying cell development, cell differentiation, and the cell cycle. Our previous studies have shown that the *GLABROUS INFLORESCENCE STEMS* (*GIS*) family genes, *GIS*, *GIS2*, and *ZINC FINGER PROTEIN8* (*ZFP8*), control shoot maturation and epidermal cell fate by integrating gibberellins (GAs) and cytokinin signaling in Arabidopsis. Here, we show that a new C2H2 zinc finger protein, ZFP5, plays an important role in controlling trichome cell development through GA signaling. Overexpression of *ZFP5* results in the formation of ectopic trichomes on carpels and other inflorescence organs. *zfp5* loss-of-function mutants exhibit a reduced number of trichomes on sepals, cauline leaves, paraclades, and main inflorescence stems in comparison with wild-type plants. More importantly, it is found that *ZFP5* mediates the regulation of trichome initiation by GAs. These results are consistent with *ZFP5* expression patterns and the regional influence of GA on trichome initiation. The molecular analyses suggest that *ZFP5* functions upstream of *GIS*, *GIS2*, *ZFP8*, and the key trichome initiation regulators *GLABROUS1* (*GL1*) and *GL3*. Using a steroid-inducible activation of *ZFP5* and chromatin immunoprecipitation experiments, we further demonstrate that *ZFP8* is the direct target of *ZFP5* in controlling epidermal cell differentiation.

Cell differentiation and morphogenesis at appropriate times and places are critical for the normal development of multicellular organisms (Ishida et al., 2008). In plants, the control of cell fate is a central issue during embryo development, meristem formation, and the transition from vegetative to reproductive phases (Szymanski et al., 2000; Schellmann et al., 2007). The regulation of cell fate requires a balance of cell proliferation and differentiation, intercellular communication, and morphogenesis control. All of these developmental processes are involved in the formation of unicellular trichomes in the shoot epidermis and root hairs in the root epidermis of Arabidopsis (*Arabidopsis thaliana*; Szymanski et al., 2000; Pesch and Hülskamp 2009). The development of trichomes and root hairs provide excellent models for the study of the molecular basis of cell specification in plants (Szymanski et al., 2000; Schiefelbein, 2003; Pesch and Hülskamp, 2004; Schellmann et al., 2007; Wang et al., 2007). Molecular and genetic analyses have been carried out in Arabidopsis to understand the regulation of cellular differentiation programs and have shown a network of transcriptional regulators that control the development of trichome and root hair in Arabidopsis (Hülskamp et al., 1994; Szymanski et al., 2000; Ishida et al., 2008; Pesch and Hülskamp, 2009). Mutant analyses, molecular protein-protein interactions, transcriptional cross-regulatory interactions, and the movement behavior of patterning genes have shown a very complicated system for trichome development (Szymanski et al., 2000; Ishida et al., 2008; Pesch and Hülskamp, 2009; Schiefelbein et al., 2009). The integration of the transcriptional regulatory network and the movement behavior enables the simulation of de novo patterning and analysis of the robustness of the system (Benítez et al., 2007, 2008; Pesch and Hülskamp, 2009). Pesch and Hülskamp (2009) have proposed the activator-inhibitor model and the activator-depletion model to explain this complicated network regulation. The key components for the activator-depletion model are the *TTG1/GLABROUS1* (*GL1*)*/MYB23/GL3/EGL3* complex. The *GL3-*

[1] This work was supported by the Zhejiang Provincial Natural Science Foundation of China (grant no. Z31100041), the National Natural Science Foundation of China (grant nos. 30970167 and 31000093), the International Scientific and Technological Cooperation Project of the Ministry of Science and Technology of China (grant no. 2010DFA34430), and the Ph.D. Programs Foundation of the Ministry of Education of China (grant no. 20090101110097).

[2] These authors contributed equally to the article.

* Corresponding author; e-mail ygan@zju.edu.cn.

The author responsible for distribution of materials integral to the findings presented in this article in accordance with the policy described in the Instructions for Authors (www.plantphysiol.org) is: Yinbo Gan (ygan@zju.edu.cn).

[C] Some figures in this article are displayed in color online but in black and white in the print edition.

[W] The online version of this article contains Web-only data.

[OA] Open Access articles can be viewed online without a subscription.

www.plantphysiol.org/cgi/doi/10.1104/pp.111.180281

Figure 1. Phenotypes of loss-of-function *zfp5* mutants and *35S:ZFP5* overexpressors. A, Main inflorescence stems (second lateral branch) of the wild type (WT; left), *35S:ZFP5* transgenic line 5 (second from left), *zfp5* (third from left), and *ZFP5:Ri* (right; *ZFP5* has been silenced by RNAi). B, Exposed floral organs from the wild type (left) and *35S:ZFP5* transgenic line 5 (right). The arrow points to ectopic trichomes. C, Rosette formation on the primary inflorescence stem of a strong *ZFP5* overexpressor. D, Trichome initiation on the second cauline leaves of *zfp5* (left) and the wild type (right). E, Trichome initiation on sepals of wild-type (left) and *zfp5* (right) flowers.

dependent depletion of *TTG1* in trichome neighboring cells results in the formulation of an activator-depletion mechanism for trichome development (Pesch and Hülskamp, 2004, 2009). It is known that the TTG1 protein moves freely and binds to GL3 in young tissues. Consequently, the cell that has more GL3 accumulates more TTG1 and becomes more competent to develop into a trichome, whereas the neighboring cells lack TTG1 and are less competent for trichome development (Pesch and Hülskamp, 2009). To date, many *GL3/GL1* direct target genes have been identified with specific expression in the very early stages of trichome initiation (Morohashi and Grotewold, 2009). The activator-inhibitor model is well supported by most researchers of trichome development in Arabidopsis.

The phytohormones GA and jasmonic acid are reported to increase trichome number and density, whereas salicylic acid decreases trichome number (Traw and Bergelson, 2003; Ishida et al., 2008). However, little information about phytohormone signaling pathways in the regulation of trichome and root hair formation is available. The first report on the involvement of GA in trichome development comes from Chien and Sussex (1996), who showed that the application of GA to the glabrous GA deficiency mutant *ga1-3* induces earlier trichome formation on the adaxial epidermis compared with the abaxial epidermis and that GA stimulates trichome formation. This result was confirmed by Telfer et al. (1997), who demonstrated the promotion of trichome production in Arabidopsis by GA and that GA regulated the abaxial trichome formation and phase change. *SPINDLY* (*SPY*) encodes a repressor of GA signaling and was first cloned by Jacobsen et al. (1996), who demonstrated that mutations of *SPY* caused a phenotype that is consistent with

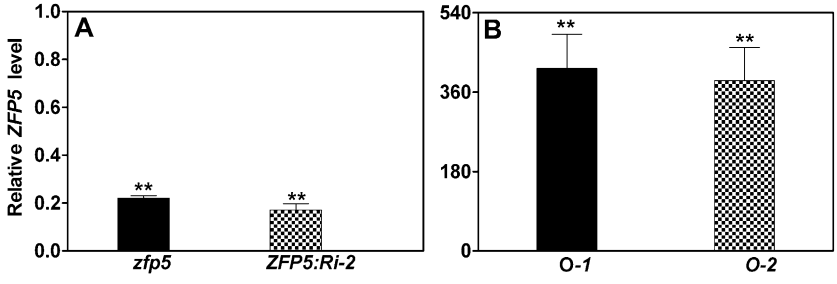

Figure 2. Relative expression levels of *ZFP5* in *zfp5* and *ZFP5:Ri-2* (A) and in *35S:ZFP5* lines *O-1* and *O-2* (B). The wild type or the corresponding control values were set at 1. LSD values were calculated at the probability of 1% (** $P < 0.01$).

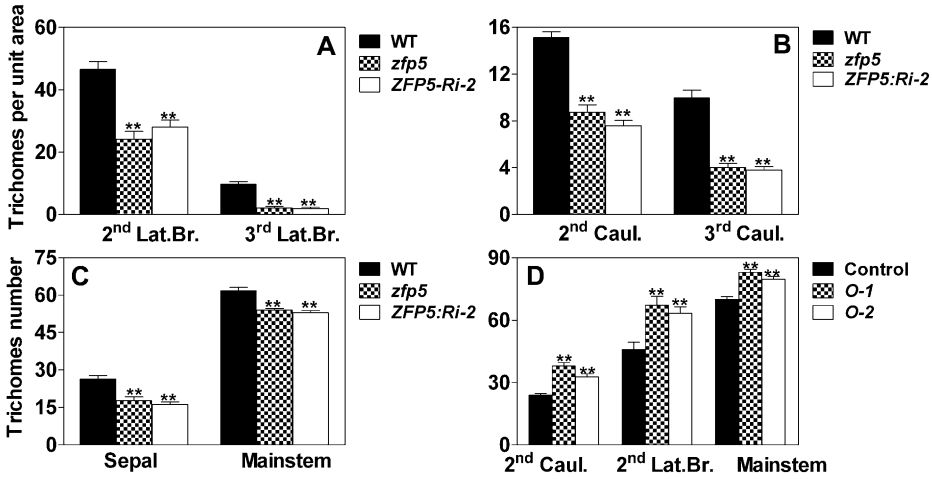

Figure 3. Trichome initiation on inflorescence organs of *zfp5*, *ZFP5*:*Ri-2*, and *35S*:*ZFP5* lines. A to C, Trichome density on the second and third branches (A), the second and third cauline leaves (B), and sepals and main stem internodes (C) in *zfp5*, *ZFP5*:*Ri-2*, and wild-type (WT) plants. D, Trichome density on inflorescence organs and rosette leaves in two *35S*:*ZFP5* lines, *O-1* and *O-2*. Caul., Cauline leaves; Lat.Br., lateral branch. Trichome number was calculated from at least 20 plants. Error bars represent SE. LSD values were calculated at the probability of 1% (** $P < 0.01$).

constitutive activation of GA signal transduction. By using the GA-deficient mutant *ga1-3*, the GA-response mutant *spy-5*, and uniconazol (a GA biosynthesis inhibitor), Perazza et al. (1998) have shown that GA-level response correlates positively with both trichome number and trichome branch number in Arabidopsis and that GA promotes trichome formation by up-regulating *GL1* in Arabidopsis. This finding was confirmed in our previous reports (Gan et al., 2006). Cytokinins also stimulate trichome formation on the inflorescence stem. GA and cytokinin signals are integrated by the C2H2 transcription factors GLABROUS INFLORESCENCE STEMS (GIS), GIS2, and ZINC FINGER PROTEIN8 (ZFP8), and they, in turn, collectively regulate *GL1* expression (Gan et al., 2006, 2007a, 2007b; Ishida et al., 2008). As we have shown previously, ZFP5 is the C2H2 transcriptional factor most closely related to the GIS clade (Gan et al., 2006); thus, the aim of this research is to determine whether *ZFP5* plays any role in the control of trichome development. Here, we report that a new C2H2 transcription factor, ZFP5, plays a key role in regulating inflorescence trichome development by directly targeting *ZFP8* expression through a GA signaling pathway.

RESULTS

Overexpression of *ZFP5* Stimulates Trichome Initiation and Causes the Heterochronic Expression of Juvenile Traits

In order to investigate whether the new C2H2 transcription factor, ZFP5, plays a role in trichome initiation, we created *35S*:*ZFP5* transgenic lines and found that they displayed an abnormally high density of trichomes on the second lateral branch (Fig. 1A) and inflorescence organs (Fig. 1B), which is similar to the phenotypes of *35S*:*GIS* and *35S*:*ZFP8* (Gan et al., 2006, 2007b). We selected two representative transgenic lines, lines 1 and 2, which exhibited high levels of *ZFP5* overexpression (Fig. 2B). Both lines had significantly more trichomes on cauline leaves, branches, and main inflorescence stems than wild-type plants (Figs. 1, A and B, and 3D). In addition, *ZFP5* overexpression caused the formation of ectopic trichomes on carpels, petals, and even stamens (Fig. 1B). Furthermore, *35S*:*ZFP5* plants also displayed a number of phenotypic changes that we explained as heterochronic shifts in development. For example, when compared with wild-type plants, *35S*:*ZFP5* plants

Table I. *zfp5 mutant, ZFP5:RNAi lines, and ZFP5 overexpressor affect plant development and inflorescence trichome initiation*

Flower trichome counts represent the total of at least 20 flowers; values are averages, and error bars correspond to SE. The trichome number on the seventh adaxial rosette leaf is counted only at the 0.72-cm^2 area in the middle of the rosette leaves. The experiment was repeated with similar results. LSD values were calculated at the probability of either 5% (* $P < 0.05$) or 1% (** $P < 0.01$). ns, Not significant; *O-1*, *35S:ZFP5*-overexpressing line 1; *O-2*, *35S:ZFP5*-overexpressing line 2.

Parameter	Wild Type	*zfp5*	*ZFP5:Ri-2*	Control	*O-1*	*O-2*
Height at maturity (cm)	16.66 ± 2.40	15.93 ± 2.25^{ns}	16.72 ± 1.83^{ns}			
Trichome no. on seventh adaxial rosette leaf	17.32 ± 2.15	16.04 ± 1.62*	14.87 ± 1.74**			
Total trichome no. on seventh abaxial rosette leaf	8.04 ± 2.64	5.04 ± 1.84**	4.17 ± 1.56**			
First leaf with abaxial trichomes	5.96 ± 0.68	5.96 ± 0.61^{ns}	6.27 ± 0.58^{ns}	6.25 ± 0.55	8.10 ± 0.64**	7.20 ± 0.52**
Total rosette leaf no. at flowering	9.92 ± 0.89	10.16 ± 1.40^{ns}	10.30 ± 0.99^{ns}	12.85 ± 0.67	17.90 ± 1.29**	14.65 ± 0.88**
Flowering time after sowing (d)	26.64 ± 0.70	26.76 ± 0.66^{ns}	26.80 ± 0.66^{ns}	28.60 ± 0.60	34.85 ± 1.73**	31.40 ± 1.6**

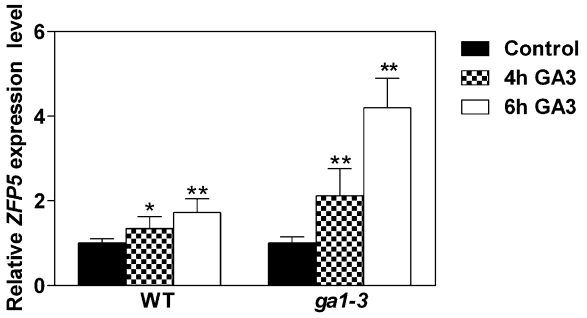

Figure 4. Expression of *ZFP5* in response to GA application. Expression of *ZFP5* was measured in inflorescence organs of wild-type (WT) and *gal-3* plants after GA treatment (100 μM) for 4 and 6 h. Transcript levels were measured by real-time PCR, and the values were normalized against the levels of *UBQ10* as a control. LSD values were calculated at the probability of either 5% (* $P < 0.05$) or 1% (** $P < 0.01$).

flowered significantly later than wild-type plants and exhibited more rosette leaves (Table I). Overexpression of *ZFP5* also caused the occasional appearance of aerial rosettes on inflorescence stems in place of cauline leaves (Fig. 1C). In conclusion, *ZFP5* overexpressors display phenotypes of a delay in shoot maturation and a strong induction of trichome production on the inflorescence.

Loss of Function of *ZFP5* Affects Inflorescence Trichome Initiation

In order to understand the involvement of *ZFP5* during trichome initiation, we selected a *zfp5* mutant (catalog no. N583960) from the Nottingham Arabidopsis Stock Centre that carries a T-DNA insertion in the *ZFP5* promoter region. The presence of T-DNA at the expected location in the *zfp5* mutant was verified by genomic PCR. We also constructed the vector in which *ZFP5* was silenced by RNA interference (RNAi; line *ZFP5*:*Ri-2*). We have generated at least six lines for *ZFP5*:*RNAi*, and all of them showed similar phenotypes. Quantitative PCR analysis showed that *ZFP5* expression was significantly suppressed in the *zfp5* mutant and *ZFP5*:*Ri-2* (Fig. 2A). To further characterize the pattern of trichome initiation in the *zfp5* mutant, we analyzed in detail the trichome distribution on stems, lateral branches, cauline leaves, and flowers in the *zfp5* mutant, *ZFP5*:*Ri-2*, and the control wild-type plants. We found that trichome initiation in the *zfp5* mutant was not affected on the first lateral branch, the first cauline leaf, and the first internode but was significantly decreased on successive stem internodes, branches, cauline leaves, and sepals (Figs. 1, D and E, and 3, A–C).

ZFP5 Controls Trichome Shoot Maturation through GA Signaling

In order to study whether *ZFP5* controls trichome initiation through GA signaling like *GIS*, we examined whether the expression level of *ZFP5* in inflorescence organs of the wild type was induced by external GA application. Wild-type and *ga1-3* mutant plants were treated with 100 μM GA, and plants were harvested at 4 and 6 h after GA application. As shown in Figure 4, *ZFP5* expression was significantly higher in GA-treated plants than in mock-treated plants in both wild-type and *ga1-3* backgrounds. This result suggests that *ZFP5* expression is induced by GA. GA is known to promote trichome initiation on leaves and inflorescence organs (Chien and Sussex, 1996; Gan et al., 2006). In order to study the response of the *zfp5* mutant to external GA application, wild-type, *zfp5*, and *ZFP5*:*RNAi-2* transgenic lines were treated with 10 and 100 μM GA shortly after flowering, as described before (Gan et al., 2006). The results showed that trichome initiation was less sensitive (the second lateral branch) than the wild type or completely insensitive (the third lateral branch and cauline leaves) to GA application in *zfp5* and *ZFP5*:*RNAi-2*. These results indicate that *ZFP5* is required for the GA signaling pathway in stimulating trichome initiation on inflorescence organs (Fig. 5, A and B).

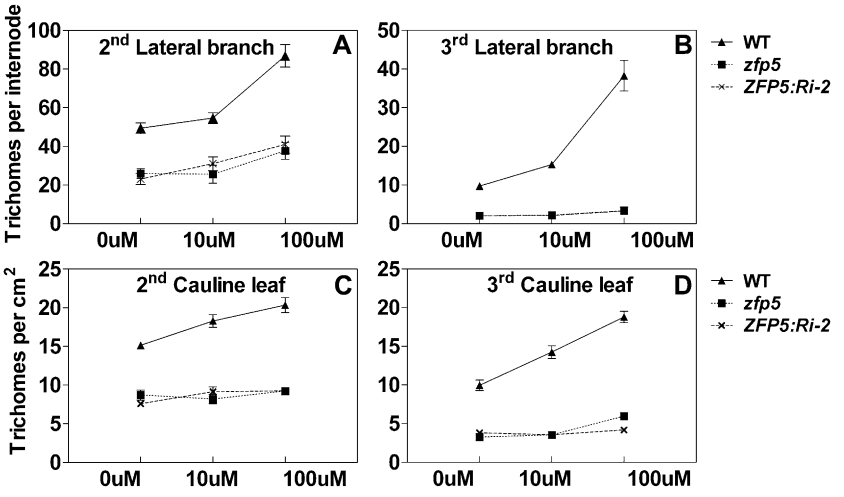

Figure 5. The effect of GA application on trichome initiation in wild-type (WT), *zfp5* mutant, and *ZFP5*:*RNAi-2* transgenic lines. Trichome initiation is shown on the inflorescence organs of wild-type, *zfp5*, and *ZFP5*:*RNAi* (termed *ZFP5*:*Ri-2*) plants that were treated with different concentrations of GA. Error bars indicate SE. The second and third lateral branches and the second and third cauline leaves were examined from 20 plants.

ZFP5 Acts Upstream of the Trichome Initiation Complex

Trichome initiation is controlled by the TTG1/GL1/MYB23/GL3/EGL3 complex, *GIS*, and its subfamily genes *GIS2* and *ZFP8*, which act downstream of *SPY* and upstream of *GL1*. To investigate the genetic position of *ZFP5* in the trichome initiation pathway, we examined the relative expression levels of *GL1*, *GL3*, *EGL3*, and *TTG1* in developing inflorescence shoots of the *zfp5* mutant and *35S:ZFP5*. We found that expression of *GL1*, *GL3*, and *EGL3* was significantly down-regulated in the *zfp5* mutant but up-regulated in *35S:ZFP5* (Fig. 6). We further overexpressed *ZFP5* in the backgrounds of *gl1*, *gl3*, and *ttg1* and revealed that the glabrous phenotype of these mutants was not rescued by overexpression of *ZFP5* (Supplemental Fig. S1, A and B). However, overexpression of a *GL3/EGL3* homologous *R* gene was able to rescue the *zfp5* mutant phenotype (Supplemental Fig. S1C). These results support that, like *GIS*, *ZFP5* acts upstream of *GL1* and *GL3/EGL3*.

ZFP5 Acts Upstream of *GIS*, *GIS2*, and *ZFP8*

Since the *zfp5* mutant showed a similar phenotype to *GIS* family mutants, the genetic position between *ZFP5* and *GIS* family genes was investigated. We examined the expression of *GIS*, *ZFP8*, and *GIS2* in *zfp5* and *35S:ZFP5*. We found that relative expression of *GIS*, *ZFP8*, and *GIS2* in the developing inflorescence shoots of *zfp5* mutants was significantly lower than in the wild-type plants but significantly higher in *35S:ZFP5* than in wild-type plants, particularly for the expression of *ZFP8* in *35S:ZFP5* (Fig. 7). Further investigation of the expression level of *ZFP5* in developing inflorescence shoots of *gis*, *gis2*, and *zfp8* mutants revealed that the expression of *ZFP5* in these mutants was not significantly different from that in wild-type plants (Supplemental Fig. S2). This result suggests that *ZFP5* functions upstream of *GIS*, *GIS2*, and *ZFP8*. To further confirm these results, we overexpressed *ZFP8* in the background of *zfp5* and revealed that the phenotype of the *zfp5* mutant was rescued by overexpression of *ZFP8* (Fig. 8). This results also suggests that *ZFP5* acts upstream of *ZFP8*.

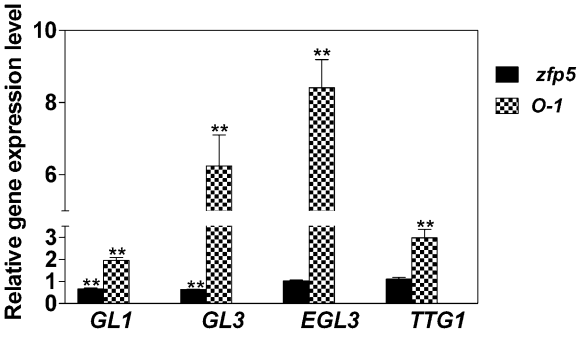

Figure 6. Relative expression of *GL1*, *GL3*, *EGL3*, and *TTG1* in developing inflorescence shoots of *zfp5* and *35S:ZFP5*. Values represent the ratios of gene expression in a particular genotype to the corresponding wild type or transgenic control. *O-1*, *35S:ZFP5*-overexpressing line 1. LSD values were calculated at the probability of 1% (** $P < 0.01$).

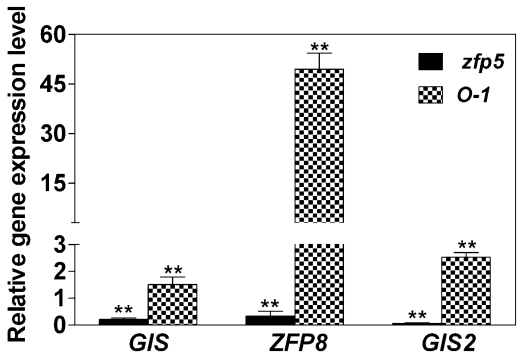

Figure 7. Relative expression of *GIS*, *ZFP8*, and *GIS2* in developing inflorescence shoots of *zfp5* and *35S:ZFP5* (*O-1*). The wild-type or the corresponding control values were set at 1. LSD values were calculated at the probability of 1% (** $P < 0.01$).

ZFP8 Is the Direct Target of *ZFP5*

To further elucidate whether *GIS*, *GIS2*, *ZFP8*, *GL1*, and *GL3* are the downstream targets of *ZFP5*, we created a steroid-inducible version of *ZFP5* in transgenic plants containing the ZFP5 protein fused to the hormone-binding domain of a rat GR under the control of a 35S promoter. Posttranslational activation of *ZFP5* can be achieved by dexamethasone (DEX) treatment of the resulting transgenic plants (Wagner et al., 1999; Yu et al., 2004). In these plants, *ZFP5* (*35S:ZFP5-GR*) activity is inducible by DEX. To validate our results, we analyzed gene expression in response to *35S:ZFP5-GR* activity in the *zfp5* mutant background. The effects of *35S:ZFP5-GR* induction were determined at different time points following DEX treatment. The results show that the expression of the key trichome initiation-positive regulators *GIS*, *GIS2*, *ZFP8*, *GL1*, and *GL3* is rapidly induced and that effect was detectable as early as 2 h after DEX application (Fig. 9). In the case of *ZFP8*, the induction was the highest, with a more than 7-fold increase. Because DEX induction of *35S:ZFP5-GR* activity does not require protein synthesis, it is possible to determine whether its effects are direct or indirect by examining the influence of protein synthesis inhibitors on induced gene expression changes (Gan et al., 2007a). To determine whether *35S:ZFP5-GR* directly or indirectly promotes trichome regulator expression, we repeated DEX applications to *35S:ZFP5-GR zfp5* in the presence of the protein synthesis inhibitor cycloheximide. We found that expression of *ZFP8* is still induced by DEX in the presence of cycloheximide, which suggests that *ZFP8* could be the direct target of *ZFP5*. Although *35S:ZFP5-GR* activity rapidly triggers the induction of trichome initiation activators *GIS*, *GIS2*, *ZFP8*, *GL1*, and *GL3*, cycloheximide treatment strongly inhibits the induction of *GIS*, *GIS2*, *GL1*, and *GL3*, which

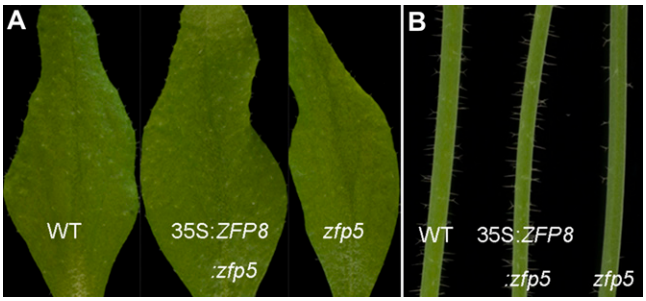

Figure 8. Overexpressed *ZFP8* restores *ZFP5* mutant trichome phenotype. A, Trichome production on cauline leaves of the wild type (WT; left), *35S:ZFP8:zfp5* (center), and *zfp5* (right). B, Trichome initiation on the second branch of the wild type (left), *35S:ZFP8:zfp5* (center), and *zfp5* (right). [See online article for color version of this figure.]

suggests that they are not the direct target of ZFP5 (Fig. 9). To further confirm whether *ZFP8* is directly regulated by *ZFP5*, we performed a chromatin immunoprecipitation (ChIP) assay using *35S:ZFP5-GFP* transgenic plants to test whether ZFP5 could bind directly to the promoter of *ZFP8*. We scanned a length of 2,055-bp *ZFP8* promoter and located four fragments spanning the conserved sequence A[AG/CT]CNAC (Fig. 10A), which were considered the C2H2 zinc finger protein-binding site of their target genes (Sakai et al., 1995; Kubo et al., 1998). Our results show that fragments I and IV are readily enriched with GFP antibody (Fig. 10B). These data further support the hypothesis that *ZFP5* is directly targeted to *ZFP8*.

ZFP5 Belongs to a Subfamily of the *GIS* C2H2 Gene Family That Is Highly Expressed in Root and at Early Stages of Inflorescence Development

Sequence analysis showed that *ZFP5* contains a C2H2 domain found in transcription factors of the TFIIIA class and is most similar to the *ZFP6* and *GIS* family of transcription factors (Meissner and Michael, 1997; Payne et al., 2004; Gan et al., 2006, 2007b). Quantitative reverse transcription (RT)-PCR analysis of *ZFP5* expression showed that *ZFP5* had a different expression pattern to that of *GIS* and its family genes *GIS2* and *ZFP8*, which were hardly detected in roots. *ZFP5* was highly expressed in roots, developing stems, branches, and young leaves but was low in rosette leaves and mature cauline leaves (Fig. 11A). We further performed in situ hybridization using a *ZFP5*-specific probe on sections of developing inflorescence stems and revealed that the gene was widely expressed in the inflorescence apex (Fig. 11B).

DISCUSSION

Functional Specialization of *ZFP5*

The surface of aerial organs in plants typically produce trichomes that have various functions against biotic and abiotic stresses in a variety of plant species, which include tobacco (*Nicotiana tabacum*), tomato (*Solanum lycopersicum*), soybean (*Glycine max*), and pepper (*Capsicum annuum*; Du et al., 2009; Harada et al., 2010; Kang et al., 2010; Kim et al., 2010). Our previous findings show that *GIS* and its related family genes *GIS2* and *ZFP8* play different roles in regulating epidermal differentiation on different aerial organs in Arabidopsis (Gan et al., 2006, 2007a). *GIS*, *ZFP8*, and *GIS2* have diverged in their responses to both developmental and hormonal signals, and these signals are not strictly interdependent (Gan et al., 2007b). The roles of *GIS*, *ZFP8*, and *GIS2* appear to be mainly in the modulation of specific epidermal responses to cytokinins and GAs. *GIS* plays a key role in controlling trichome initiation on inflorescence stems, *GIS2* mainly controls trichome initiation on inflorescence flowers, while *ZFP8* is the key regulator for trichome initiation on cauline leaves (Gan et al., 2006, 2007b). As we reported before, although the *GIS*, *ZFP8*, and *GIS2* genes are functionally equivalent proteins, they have diverged in their responses to plant hormones and in their roles during inflorescence development (Gan et al., 2006, 2007b). As the expression patterns of *GIS*, *ZFP8*, and *GIS2* are different and both the roles and inducibility of the genes in response to cytokinins are clearly different, we suggest that GIS, ZFP8, and GIS2 have diverged in their responses to both developmental and hormonal signals and that these signals are not strictly interdependent (Gan et al., 2007b). Thus, there could be two different pathways: one where GIS controls trichome development mainly by the regulation of expression of *GL1/GL3* (Gan et al., 2006, 2007b) through GA, and another, the GIS2/ZFP8 pathway, which integrates both GA and cytokinin signals to control trichome development in inflorescence organs (Gan et al., 2007b).

In this study, *ZFP5* differs from the *GIS* clade, which plays a general role in modulating growth and differentiation in response to GA signals (Achard et al., 2003, 2006; Fu and Harberd, 2003; Gan et al., 2006, 2007a,

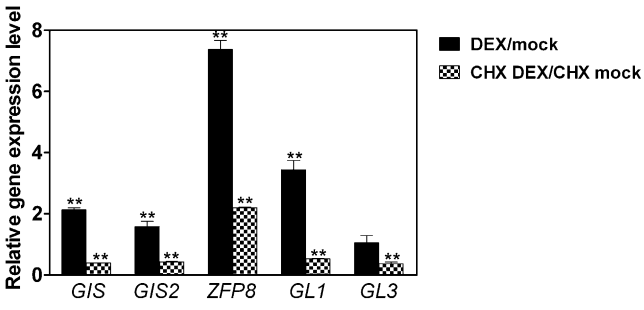

Figure 9. Induced ZFP5 activity can transcriptionally activate the expression of *GIS*, *GIS2*, *ZFP8*, *GL1*, and *GL3*, and *ZFP8* is the direct target of *ZFP5*. Quantitative RT-PCR analysis is shown for RNA from the *zfp5* mutant harboring ZFP5: GR treated with 10 μM DEX for 2 h (black bars) and treated with 10 μM DEX and 20 μM CHX for 2 h (hatched bars). Values are averages, and error bars correspond to SE. LSD values were calculated at the probability of 1% (** $P < 0.01$).

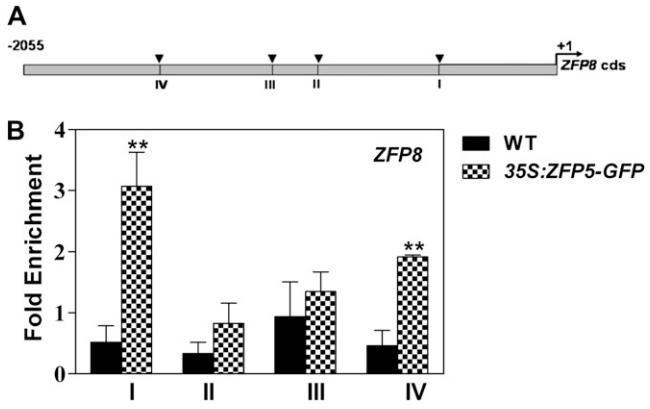

Figure 10. ChIP analysis of *ZFP8* promoter regions bound by *35S:ZFP5-GFP*. A, Schematic diagram of the *ZFP8* promoter. The arrowheads indicate the sites containing either a single mismatch or a perfect match from the consensus binding sequence A[AG/CT]CNAC for C2H2 zinc finger proteins. B, Quantitative real-time PCR assay of DNAs after ChIP. *TUBULIN2* was used as a reference, and the primer used was described by Yu et al. (2010). Values are averages, and error bars correspond to SE. LSD values were calculated at the probability of 1% (** $P < 0.01$). WT, Wild type.

2007b). It appears that *ZFP5* plays a predominant role in trichome initiation on inflorescence stems and cauline leaves (Figs. 1, D and E, and 3, B and C). Our genetic and molecular analyses have shown that *ZFP5* acts upstream of the trichome key positive regulators *GL1*, *GL3*, *GIS*, *GIS2*, and *ZFP8* by directly targeting *ZFP8* (Fig. 10). Therefore, *ZFP5* highlights the key role played by transcription factors not only upstream of the *GIS* clade but also downstream of hormone production (Fig. 12). The model of *ZFP5* controlling epidermal cell differentiation is summarized in Figure 12. These results will provide a better understanding of how developmental and hormonal signals are integrated in plants by transcription factors. A recent report from Yu et al. (2010) demonstrates that the SQUAMOSA PROMOTER-BINDING PROTEIN-LIKE gene *SPL9*, which is targeted by microRNA156 (miR156), plays a key role in controlling inflorescence trichome development by directly targeting *TRY* and *TCL1*. Yu et al. (2010) further demonstrated that *miR156/SPL* is not related to the GIS-dependent pathway and that these two pathways function in parallel in regulating the trichome regulator complex in the main stem and inflorescences. Since *ZFP5* belongs to a subfamily gene of the GIS C2H2 family and acts upstream of the *GIS* gene family by directly regulating *ZFP8*, it is unlikely to play any role in the miR156/SPL-dependent pathway. Since our gene expression data have shown clearly that *ZFP5* is highly expressed in the root, further study is needed to determine whether *ZFP5* plays a role in the control of root or root hair development.

ZFP5 Regulates Phase Change

As we reported before, the heterochronic phenotype of *GIS*, *GIS2*, and *ZFP8* overexpressors and loss-of-function mutants suggested that *GIS*, *GIS2*, and *ZFP8* influence trichome initiation as part of a more general role in the regulation of phase change (Gan et al., 2006, 2007b). In order to test whether *ZFP5* plays a role in this phase change, we first investigated the phenotype resulting from the overexpression of *ZFP5*. The results showed that the *ZFP5* overexpressor delays flowering time and the transition period from vegetative stage to reproductive stage (Table I), which suggests that *ZFP5* may play a general role in regulating phase change. We further examined the process of shoot maturation in the *zfp5* mutant. We found that the mutation did not affect flowering time in long days or the adaxial leaf number, but it significantly affected the abaxial leaf number of the rosette leaves (Table I). These results suggested that a loss of *ZFP5* function not only affects epidermal differentiation after floral induction under normal growth conditions but also plays a role in phase change. Elucidating how increases in *GIS* activity and its family genes influence phase change will require further investigation.

In summary, we have cloned and characterized a new C2H2 zinc finger protein, ZFP5, which plays a key role in

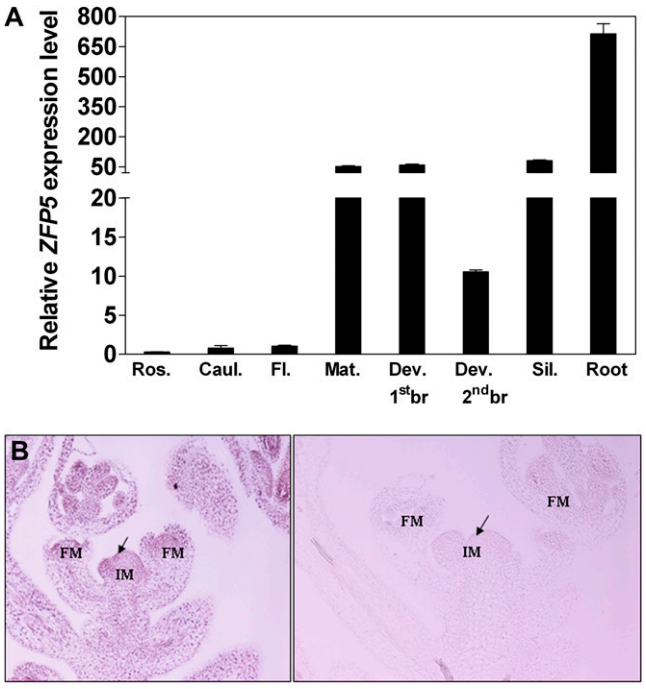

Figure 11. Expression pattern of the *ZFP5* gene. A, Quantitative RT-PCR analysis of *ZFP5* expression in different tissues of wild-type plants. All values are normalized using an internal standard (*UBQ10*). Ros., Rosette leaf; Caul., cauline leaf; Fl., flower; Mat. stem, fully elongated first internode of the main stem; Dev. 1st br., the first developing branch (lateral branch); Dev. 2nd br., the second developing branch (lateral branch); Sil., silique. B, In situ hybridization of *ZFP5* probes to developing inflorescence shoot sections. *ZFP5* is expressed broadly in stems and inflorescence meristems (IM) and strongly in floral meristems (FM). The section hybridized with the antisense probe is shown on the left, while the one hybridized with the sense probe is shown on the right.

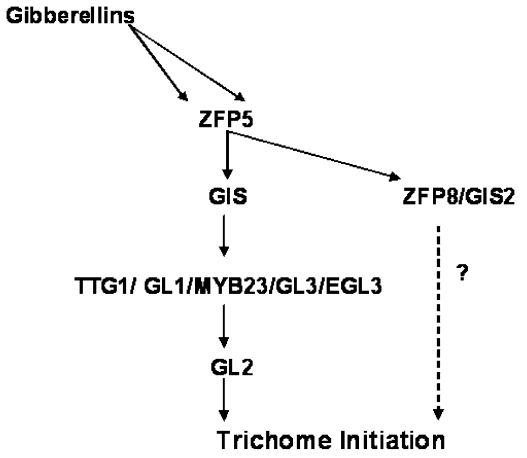

Figure 12. Model of *ZFP5* action in Arabidopsis inflorescence organs in response to GA.

shoot maturation and trichome initiation in the inflorescence organs. Our results clearly demonstrated that *ZFP5* controls shoot maturation by regulating the expression of *GIS*, *GIS2*, *ZFP8*, *GL1*, and *GL3* through integrating GA signaling by directly targeting *ZFP8* (Fig. 10). This is another big step for us to better understand the transcriptional factor controlling trichome initiation by integrating GA signal. Since there are two more genes, *ZFP6* and *At1g68360* (Gan et al., 2006), in the *ZFP5* clade, the cloning and characterization of these two genes should bring further insights into this mode of action for the transcriptional factors controlling shoot maturation and trichome cell differentiation by integrating plant hormones and environmental cues.

MATERIALS AND METHODS

Plant Materials and Growth Conditions

Arabidopsis (*Arabidopsis thaliana*) ecotype Columbia was used as a control for most experiments in this study. The plants were grown in a controlled growth room with the following growth conditions: 20°C to 22°C, 90 to 120 μmol m^{-2} s^{-1}, 16/8-h photoperiod, and 68% to 78% humidity. For in the vitro experiments, seeds were surface sterilized with 5% (v/v) NaClO solution for 7 min and washed five times in sterile distilled water, plated on Murashige and Skoog medium and vernalized at 4°C for 3 d in the dark, and then placed in a growth room.

Isolation of a *zfp5* Loss-of-Function Mutant

A transgenic line (catalog no. N583960) carrying a T-DNA insertion in the *ZFP5* promoter was identified in the Nottingham Arabidopsis Stock Centre line collection. Homozygous mutants were selected by ensuring that all of their progeny were resistant to kanamycin (50 mg L^{-1}). The presence of the T-DNA insertion was confirmed by PCR using gene-specific primers (5′ primer, 5′-TGTGACGAGAAATGATCTTGG-3′; 3′ primer, 5′-ATAGATGCTTGCATCATTGCC-3′) and a T-DNA insertion primer (5′-ATTTTGCCGATTTCGGAAC-3′).

Cloning

For all cloning constructs (*35S:ZFP5*, *ZFP5:RNAi*,), sequences were first inserted into the pENTR-1A vector (Invitrogen) before being recombined into an appropriate destination vector using the Gateway LR reaction (Invitrogen). All destination vectors were obtained from the Flanders Interuniversity Institute for Biotechnology as described before (Gan et al., 2006). pH2GW7 was used for preparing the *35S:ZFP5* construct, pK7GWIWG2(II), for the *ZFP5:RNAi* construct. For all these cloning experiments, gene-specific fragments were first PCR amplified from cDNA (*35S:ZFP5*, *ZFP5:RNAi*) using primers containing *Sal*I and *Not*I restriction sites and purified using a gel extraction kit (Qiagen) before restriction and cloning. The following primers were used: *ZFP5* overexpression, 5′-CGGTCGACATGTCTATAAATCCG-3′ and 5′-AAGCGGCCGCTGCCGCATCTCCGGCA-3′; *ZFP5:RNAi*, 5′-CGGTCGACGAGCCAGCATCGGCTATTAT-3′ and 5′-AAGCGGCCGCAATTTGTTATGCCGCATCTCC-3′. For all of the genetic transgenic experiments, the constructs in binary vectors were transformed into *Agrobacterium tumefaciens* GV3101 strain, which were then used to transform Arabidopsis with the appropriate genotype background using the floral-dip method as described by Clough and Bent (1998). Transgenic seedlings were first selected on Murashige and Skoog agar plates with appropriate antibiotics and then confirmed by PCR using the corresponding primers. We created *35S:ZFP5-GR* using a derivative pGreen0244 vector (pGreen0244:GR donated by Prof. Hao Yu). The entire *ZFP5* cDNA was amplified by RT-PCR with the primers *ZFP5-LP* (5′-CACTACGCGTATGTCTATAAATCCGACAAT-3′) and *ZFP5-RP* (5′-TAATGGGCCCTGCCGCATCTCCGGCAAAAC-3′). The resulting fragment was digested by *Apa*I and *Mlu*I sites of pGreen0244 and subsequently cloned into the corresponding sites of pGreen0244 to generate *35S:ZFP5-GR*.

GA Treatments and Gene Expression Analysis

GA_3 (Sigma) was used in all experiments that involved exogenous GA treatments, as described previously (Gan et al., 2006, 2007b). For measuring the effect of GA applications on gene expression, a minimum of eight mutant and control plants were grown on soil until young inflorescence shoots had reached a size of 2 to 3 cm. The plants were then sprayed with either 100 μM GA_3 or a mock solution, and the shoots were harvested 4 and 6 h (GA) after treatment for RNA extraction (Gan et al., 2006).

RNA Extraction and Real-Time PCR

The total RNA was extracted from Arabidopsis organs with TRIzol Reagent (Invitrogen), and cDNA was synthesized from 1.5 μg of total

Table II. *Primer pairs used for ChIP assays*

Gene	Sequence (5′–3′)	Purpose
ZFP8 chip LP1	TCCTATGCTTCCATACGCTAA	ChIP, region I
ZFP8 chip RP1	TGACTCCATGGTGCATGTTT	ChIP, region I
ZFP8 chip LP2	AACCAAATAGGTCCGTGATGTT	ChIP, region II
ZFP8 chip RP2	AGCAGATGAAATGGGGTCAC	ChIP, region II
ZFP8 chip LP3	TCATGAACATGGACCACCTC	ChIP, region III
ZFP8 chip RP3	GGATGTTTTGTCTCTTTGATGC	ChIP, region III
ZFP8 chip LP4	CCGCTCAAAACAACTAACTGAA	ChIP, region IV
ZFP8 chip RP4	TTTGACGACTCCCAAATTCC	ChIP, region IV
TUB2 chip LP	TAAATTCTGAACCCATTGTTTCTCA	Control
TUB2 chip RP	AGTCCGATGATTGGCTTTATTATTC	Control

RNA using Moloney murine leukemia virus transcriptase (Promega) and oligo(dT)$_{18}$ primers in a 25-μL reaction according to the manufacturer's instructions. For real-time PCR, the cDNAs were diluted to 100 μL, and 2 μL was added to 12.5 μL of SYBR Green PCR mix (Takara) and 0.5 μL of each primer (200 nM final concentration) in 25-μL reactions. PCR and detection were performed using a Stratagene M×3005P thermal cycler using the following cycling conditions: 95°C for 1 min, followed by 40 cycles of 95°C for 5 s and 60°C for 20 s. Optimization experiments were performed to establish the optimal PCR programs. Melting-curve analysis was used to confirm the absence of nonspecific amplification products. *UBQ10* transcripts were used as an endogenous control to normalize expression of the other genes according to Gan et al. (2006). Relative expression levels were calculated by subtracting the threshold cycle (Ct) values for *UBQ10* from those of the target gene (to give ΔCt) and then calculating $2^{-\Delta Ct}$ as described previously (Gan et al., 2005). RT-PCR experiments were performed on at least three independent samples.

In Situ Hybridization

Nonradioactive in situ hybridization was performed as described previously (Gan et al., 2006). For synthesis of the *ZFP5* RNA probes, gene-specific fragments were amplified using the same primers as for generating the RNAi constructs (see above).

DEX Treatment

For the *35S:ZFP5-GR* transgenic line selection, we screened for a transgenic line that contains only one transgene insertion and that exhibits a phenotype closely resembling *35S:ZFP5*. The DEX treatment and sample collection were the same as described by Yu et al. (2004) and Wagner et al. (1999). Relative expression levels were calculated according to Yi et al. (2010). *UBQ10* transcripts were used as an endogenous control to normalize expression of the other genes. Quantitative RT-PCR experiments were performed at least on three independent samples.

ChIP

ChIP assays were carried out as described by Yu et al. (2010). About 3 g of tissues of 4-week-old *35S:ZFP5-GFP* plants and wild-type plants were harvested and fixed in 15.4 mL of fixation buffer (0.4 M Suc, 10 mM Tris, pH 8.0, 1 mM EDTA, pH 7.5, 1 mM phenylmethylsulfonyl fluoride, and 1% formaldehyde). After fixation, the material was washed four times with double distilled water and ground under liquid nitrogen. The resultant powder was added to 10 mL of extraction buffer (0.4 M Suc, 10 mM Tris-HCl, pH 8.0, 10 mM $MgCl_2$, 5 mM mercaptoethanol, 0.1 mM phenylmethylsulfonyl fluoride, and 1× protease inhibitor [Roche]), vortexed to mix, kept at 4°C until the solution was homogenous, and then rotated for 20 min at 4°C. After that, the pellet was resuspended with lysis buffer (50 mM HEPES, pH 7.5, 150 mM NaCl, 1 mM EDTA, 1% Triton X-100, 0.1% deoxycholate sodium, and 0.1% SDS) and sonicated with an ultrasonic cell disruptor (JY96-II [output 3 and 6 × 10 s]; Xinzhi). The solution was divided into three parts: one was saved as total DNA without precipitation, and other two parts were incubated with either an anti-GFP antibody (Abmart) or an anti-hemagglutinin antibody (Abmart) , the latter of which was precipitated in parallel as a negative control. The resulting DNA samples were purified with a PCR purification kit (Qiagen). The relative concentrations of the DNA fragments were analyzed by quantitative real-time PCR using the *β-TUBULIN2* gene promoter as the reference, and DNA enrichment was examined by quantitative real-time PCR in triplicate as described previously (Jun et al., 2010; Yu et al., 2010). All primers used in the ChIP assays are listed in Table II.

Statistical Analyses

All data in Table I were tested by means of ANOVA for significance by using the Statistix program version 3.5 (Analytical Software). LSD values were calculated at either 5% ($P < 0.05$) or 1% ($P < 0.01$) probability as we described before (Gan et al., 2010).

Sequence data from this article can be found in the GenBank/EMBL data libraries under the following accession numbers: *ZFP5* (At1g10480), *GIS* (At3g58070), *GIS2* (At5g06650), *ZFP8* (At2g41940), *GL1* (At3g27920), *GL3* (At5g41315), *EGL3* (At1g63650), *TTG1* (At5g24520), *TUB2* (At5g62690), and *UBQ10* (At4g05320).

Supplemental Data

The following materials are available in the online version of this article.

Supplemental Figure S1. Genetic interaction between *ZFP5* and key trichome initiation complex genes.

Supplemental Figure S2. *ZFP5* expression in developing inflorescence shoots of *gis*, *zfp8*, and *gis2*.

ACKNOWLEDGMENTS

We thank Dr. Clare Steele-King (University of York) for critical reading of the manuscript and Prof. Alan Lloyd (University of Texas at Austin) for providing the *gl3-1* mutant. Technical assistance and help with the ChIP experiment from Dr. Nan Yu and Dr. Wenjuan Cai of Prof. Xiaoya Chen's laboratory (Shanghai Institute for Biological Science) are gratefully acknowledged.

Received May 24, 2011; accepted July 28, 2011; published July 29, 2011.

LITERATURE CITED

Achard P, Cheng H, De Grauwe L, Decat J, Schoutteten H, Moritz T, Van Der Straeten D, Peng J, Harberd NP (2006) Integration of plant responses to environmentally activated phytohormonal signals. Science **311:** 91–94

Achard P, Vriezen WH, Van Der Straeten D, Harberd NP (2003) Ethylene regulates *Arabidopsis* development via the modulation of DELLA protein growth repressor function. Plant Cell **15:** 2816–2825

Benítez M, Espinosa-Soto C, Padilla-Longoria P, Alvarez-Buylla ER (2008) Interlinked nonlinear subnetworks underlie the formation of robust cellular patterns in *Arabidopsis* epidermis: a dynamic spatial model. BMC Syst Biol **2:** 98–113

Benítez M, Espinosa-Soto C, Padilla-Longoria P, Diaz J, Alvarez-Buylla ER (2007) Equivalent genetic regulatory networks in different contexts recover contrasting spatial cell patterns that resemble those in *Arabidopsis* root and leaf epidermis: a dynamic model. Int J Dev Biol **51:** 139–155

Chien JC, Sussex IM (1996) Differential regulation of trichome formation on the adaxial and abaxial leaf surfaces by gibberellins and photoperiod in *Arabidopsis thaliana* (L.) Heynh. Plant Physiol **111:** 1321–1328

Clough SJ, Bent AF (1998) Floral dip: a simplified method for Agrobacterium-mediated transformation of *Arabidopsis thaliana*. Plant J **16:** 735–743

Du WJ, Yu DY, Fu SX (2009) Analysis of QTLs for the trichome density on the upper and downer surface of leaf blade in soybean Glycine max (L.) Merr. Agric Sci China **8:** 529–537

Fu X, Harberd NP (2003) Auxin promotes Arabidopsis root growth by modulating gibberellin response. Nature **421:** 740–743

Gan Y, Filleur S, Rahman A, Gotensparre S, Forde BG (2005) Nutritional regulation of ANR1 and other root-expressed MADS-box genes in *Arabidopsis thaliana*. Planta **222:** 730–742

Gan Y, Kumimoto R, Liu C, Ratcliffe OJ, Yu H, Broun P (2006) GLABROUS INFLORESCENCE STEMS modulates the regulation by gibberellins of epidermal differentiation and shoot maturation in *Arabidopsis*. Plant Cell **18:** 1383–1395

Gan Y, Yu H, Peng J, Broun P (2007a) Genetic and molecular regulation by DELLA proteins of trichome development in Arabidopsis. Plant Physiol **145:** 1031–1042

Gan Y, Zhou Z, An L, Bao S, Liu Q, Srinivasa M, Goddard P (2010) The effects of fluctuations in the nutrient supply on the expression of ANR1 and 11 other MADS box genes in shoots and roots of *Arabidopsis thaliana*. Botany **88:** 1023–1031

Gan YB, Liu C, Yu H, Broun P (2007b) Integration of cytokinin and gibberellin signalling by *Arabidopsis* transcription factors GIS, ZFP8 and GIS2 in the regulation of epidermal cell fate. Development **134:** 2073–2081

Harada E, Kim JA, Meyer AJ, Hell R, Clemens S, Choi YE (2010) Expression profiling of tobacco leaf trichomes identifies genes for biotic and abiotic stresses. Plant Cell Physiol **51:** 1627–1637

Hülskamp M, Misŕa S, Jürgens G (1994) Genetic dissection of trichome cell development in *Arabidopsis*. Cell **76:** 555–566

Ishida T, Kurata T, Okada K, Wada T (2008) A genetic regulatory network in the development of trichomes and root hairs. Annu Rev Plant Biol **59:** 365–386

Jacobsen SE, Binkowski KA, Olszewski NE (1996) SPINDLY, a tetratricopeptide repeat protein involved in gibberellin signal transduction in Arabidopsis. Proc Natl Acad Sci USA **93:** 9292–9296

Jun JH, Ha CM, Fletcher JC (2010) BLADE-ON-PETIOLE1 coordinates organ determinacy and axial polarity in *Arabidopsis* by directly activating ASYMMETRIC LEAVES2. Plant Cell **22:** 62–76

Kang JH, Liu GH, Shi F, Jones AD, Beaudry RM, Howe GA (2010) The tomato odorless-2 mutant is defective in trichome-based production of diverse specialized metabolites and broad-spectrum resistance to insect herbivores. Plant Physiol **154:** 262–272

Kim HJ, Han JH, Kwon JK, Park M, Kim BD, Choi D (2010) Fine mapping of pepper trichome locus 1 controlling trichome formation in Capsicum annuum L. CM334. Theor Appl Genet **120:** 1099–1106

Kubo K, Sakamoto A, Kobayashi A, Rybka Z, Kanno Y, Nakagawa H, Takatsuji H (1998) Cys2/His2 zinc-finger protein family of petunia: evolution and general mechanism of target-sequence recognition. Nucleic Acids Res **26:** 608–615

Meissner R, Michael AJ (1997) Isolation and characterisation of a diverse family of Arabidopsis two and three-fingered C2H2 zinc finger protein genes and cDNAs. Plant Mol Biol **33:** 615–624

Morohashi K, Grotewold E (2009) A systems approach reveals regulatory circuitry for *Arabidopsis* trichome initiation by the GL3 and GL1 selectors. PLoS Genet **5:** e1000396

Payne T, Johnson SD, Koltunow AM (2004) KNUCKLES (KNU) encodes a C2H2 zinc-finger protein that regulates development of basal pattern elements of the *Arabidopsis* gynoecium. Development **131:** 3737–3749

Perazza D, Vachon G, Herzog M (1998) Gibberellins promote trichome formation by up-regulating GLABROUS1 in Arabidopsis. Plant Physiol **117:** 375–383

Pesch M, Hülskamp M (2004) Creating a two-dimensional pattern de novo during *Arabidopsis* trichome and root hair initiation. Curr Opin Genet Dev **14:** 422–427

Pesch M, Hülskamp M (2009) One, two, three...models for trichome patterning in *Arabidopsis*? Curr Opin Plant Biol **12:** 587–592

Sakai H, Medrano LJ, Meyerowitz EM (1995) Role of SUPERMAN in maintaining Arabidopsis floral whorl boundaries. Nature **378:** 199–203

Schellmann S, Hülskamp M, Uhrig J (2007) Epidermal pattern formation in the root and shoot of *Arabidopsis*. Biochem Soc Trans **35:** 146–148

Schiefelbein J (2003) Cell-fate specification in the epidermis: a common patterning mechanism in the root and shoot. Curr Opin Plant Biol **6:** 74–78

Schiefelbein J, Kwak SH, Wieckowski Y, Barron C, Bruex A (2009) The gene regulatory network for root epidermal cell-type pattern formation in *Arabidopsis*. J Exp Bot **60:** 1515–1521

Szymanski DB, Lloyd AM, Marks MD (2000) Progress in the molecular genetic analysis of trichome initiation and morphogenesis in *Arabidopsis*. Trends Plant Sci **5:** 214–219

Telfer A, Bollman KM, Poethig RS (1997) Phase change and the regulation of trichome distribution in Arabidopsis thaliana. Development **124:** 645–654

Traw MB, Bergelson J (2003) Interactive effects of jasmonic acid, salicylic acid, and gibberellin on induction of trichomes in Arabidopsis. Plant Physiol **133:** 1367–1375

Wagner D, Sablowski RW, Meyerowitz EM (1999) Transcriptional activation of APETALA1 by LEAFY. Science **285:** 582–584

Wang SC, Kwak SH, Zeng QN, Ellis BE, Chen XY, Schiefelbein J, Chen JG (2007) TRICHOMELESS1 regulates trichome patterning by suppressing GLABRA1 in *Arabidopsis*. Development **134:** 3873–3882

Yi K, Menand B, Bell E, Dolan L (2010) A basic helix-loop-helix transcription factor controls cell growth and size in root hairs. Nat Genet **42:** 265–267

Yu H, Ito T, Zhao Y, Peng J, Kumar P, Meyerowitz EM (2004) Floral homeotic genes are targets of gibberellin signaling in flower development. Proc Natl Acad Sci USA **101:** 7827–7832

Yu N, Cai WJ, Wang SC, Shan CM, Wang LJ, Chen XY (2010) Temporal control of trichome distribution by microRNA156-targeted SPL genes in *Arabidopsis thaliana*. Plant Cell **22:** 2322–2335